Implementing a gradient dependent plasticity model in ABAQUS

ARTICLE · JANUARY 2007

1 AUTHOR:

Lars Pilgaard Mikkelsen
Technical University of Denmark

Implementing a gradient dependent plasticity model in ABAQUS

Lars Pilgaard Mikkelsen

Material Research Department, Risø National Laboratory,
Technical University of Denmark, DK-4000 Roskilde, Denmark

Abstract: A strain gradient dependent plasticity model is implemented using the user element subroutine interface in ABAQUS. Based on the implementation, a simple shear case is studied as well as a more complex crack tip problem. Large influence of the incorporated material length scale is observed in the two cases.

Keywords: Constitutive laws, Strain gradient plasticity, Length scale effects, User elements

1. Introduction

The microstructure of a material is not taken into account in conventional plasticity theories as those theories consider the material as a homogeneous material. Therefore, no scale effect can be predicted. On the other hand, modeling the actual microstructure of the material can be a comprehensive and tedious work exposing a great deal of unnecessary details. Nevertheless by include the effects of the underlying microstructure in an averaging way using material length scales; it is possible to predict the influence of e.g. deformation localization or crack growth on the macroscopic structural behavior and/or to include scale effect in finite element studies of mechanical devices on the micron scale. This is what has been done in many of the recently proposed gradient dependent plasticity theories (Aifantis, 1984, Echarya and Bassani, 2000, Fleck and Hutchinson, 1997)

A large number of experiments has shown length scale effects in materials. E.g. has Fleck *et al.*, 1994 shown that twisting a thin copper wires with a diameter going from $100\mu m$ to $12\mu m$ results in a stiffer response where the normalized torque increase with a factor of three. Similar, has Stelmashenko *et al.*, 1993 shown that using a micro indenter with a diameter going from $100\mu m$ to $2\mu m$ results in an increase in the measured stiffness with a factor of 2. Both cases show a length scale effects which a conventional plasticity theory can not capture as no information regarding the microstructure of the underlying material is incorporated in a standard model.

In the presented work, a strain gradient plasticity theory (Fleck and Hutchinson, 2001) has been implemented in ABAQUS. Using this theory, three length scales is incorporated in the model. In the finite element model, both the displacement increments and the increments of the effective plastic strain are taken as fundamental unknowns. Therefore, the model is implemented in a user element subroutine. The model has been used to reveal the applicability of the theory on a number of test cases as well as to model length scale effects on crack growth simulations at elastic/elastic-plastic material interfaces using cohesive elements. Results demonstrating length scale effects as well as applicability of higher order boundary condition. In addition, it is shown that strain gradient plasticity theories is crucial for realistic crack growth prediction along strong elastic/elastic-plastic interfaces.

2. Gradient dependent J_2-flow theory

A power-law hardening material law is used where the tangent modulus depends on a gradient dependent effective plastic strain

$$\dot{E}^{P^2} = \dot{\varepsilon}^{P^2} + A_{ij}\dot{\varepsilon}^P_{,i}\dot{\varepsilon}^P_{,j} + B_{,i}\dot{\varepsilon}^P_{,i}\dot{\varepsilon}^P + C\dot{\varepsilon}^{P^2} \tag{1}$$

The coefficients A_{ij}, B_i and C, see Fleck and Hutchinson (2001) depends on three material length scales, ℓ_1, ℓ_2, ℓ_3, the outward normal the plastic yield, $m_{ij} = (3/2)\, s_{ij} / \sigma_e$, and the gradient thereof, $m_{ij,k}$. A one length scale version, ℓ_*, which can be considered as a special case of (1) has been formulated as

$$\dot{E}^{P^2} = \dot{\varepsilon}^{P^2} + \ell_* \dot{\varepsilon}^P_{,i}\dot{\varepsilon}^P_{,i} \tag{2}$$

Both the three and one material length scale version of the theory is prescribed in detailed in Fleck and Hutchinson (2001) and will not be repeated here. In addition to the higher order plastic strains, $\dot{\varepsilon}^P_{,j}$, the model introduce the corresponding higher order stresses, τ_i, (work conjugated to $\dot{\varepsilon}^P_{,j}$) and higher order boundary condition, see Fleck and Hutchinson (2001). E.g. is it possible to prescribe the boundary condition $\dot{\varepsilon}^P = 0$ which for a metal plasticity corresponds to a boundary where the dislocations can not penetrate, e.g. on a boundary to an elastic material. The hardening of the material is in the present work given by a standard power-law hardening such that the materials hardening modulus is given by

$$h[E^P] = \left(\frac{EE_T[E^P]}{E - E_T[E^P]} \right) \text{ where } E_T[E^P] = \frac{E}{n}\left(\frac{EE^P}{\sigma_y} + 1 \right)^{\frac{1}{n}-1} \tag{3}$$

where E denote Young's modulus, σ_y the initial yield stress and n the hardening exponent. Note that in equation (3), the hardening modulus depends on the gradient dependent effective plastic strain E^P from equation (1) or (2) and not the conventional effective plastic strain ε^P_e.

3. Numerical implementation in ABAQUS

The implementation of the strain gradient dependent plasticity model is inspired by Niordson and Hutchinson (2003) and many details regarding the implementation can be found there. Contrary to Niordson and Hutchinson (2003), the presented work implement the model in the user subroutine interface Uel in the commercial finite element code ABAQUS. In the finite element implementation, both the nodal displacement increments $\dot{U}_i^n$ and the nodal increment of the effective plastic strain $\dot{\varepsilon}_n^{\,P}$ are taken as fundamental unknowns.

$$\dot{u}_i = \sum_{n=1}^{2k} N_i^n \dot{U}^n \quad \text{and} \quad \dot{\varepsilon}^p = \sum_{n=1}^{l} M^n \dot{\varepsilon}_n^p \tag{4}$$

where $N_i^{\,n}(x_j)$ and $M_i^{\,n}(x_j)$ are shape functions defined such that equation (4) gives their respectively values in the point x_j inside the element. In the presented implementation, both the increment of the displacement and the increment of the effective plastic strain have been modeled using standard isoparametric shape functions. Nevertheless, the isoparametric element used to discretize the displacements increments and the effective plastic strain do not necessary include the same number of nodes. Later the best performance is found for an element with $k=8$ and $l=4$. Substitute (4) into the virtual work on incremental form, see Niordson and Hutchinson (2003) results in the system of linear equitation shown in (5)

$$\begin{bmatrix} K_e & K_{ep} \\ K_{ep}^{\;T} & K_p \end{bmatrix} \begin{bmatrix} \dot{U} \\ \dot{\varepsilon}^P \end{bmatrix} = \begin{bmatrix} \dot{F}_1 \\ \dot{F}_2 \end{bmatrix} + \begin{bmatrix} C_1 \\ 0 \end{bmatrix} \tag{5}$$

where $\dot{U}$ and $\dot{\varepsilon}^P$ are the fundamental unknowns in the finite element model. The term C_1 is the equilibrium term from where the unbalanced nodal forces can be extracted and from where ABAQUS found equilibrium when other element from ABAQUS is included in the model. The model is implemented as an plane strain version.

The procedure when calling the Uel is as following:

1. Based on the tangent stiffness in the beginning of the increment, all the state variable is updated.
2. Decide whether or not the material point will begin to yield or elastically unload in the next increment.
3. Calculate the element stiffness matrix based on the updated state variable (the stiffness in the end of the increment and return to ABAQUS.

3.1 Using the element en ABAQUS

An example on the input to the user element is shown below.

```
** Variables=56, 126, 224
*** 4-noded plane strain elements
*user element, type=u1, nodes=8, coordinates=2,properties=21,i properties=0,
variables=126
1,2,11
5,1,2
*Element, type=u1, elset=Model
  1,1,2,3,4,5,6,7,8
....
....
*uel property, elset=Model
** Emod, Enu, Sig0, nhard, thick, igrad, lgrad1,lgrad2
    1,   0.3, 0.01,   5,    1.0,    1,     1,    0,
** lgrad3,depsmax,dyield, fhrad
    0,    1e-3,   1e-5,   1e5
```

In here, the variable=56, 126 or 224 decide whether there is used an 2x2, 3x3 or 4x4 integration scheme. The two lines

```
1,2,11
5,1,2
```

prescribe the first 4 nodes to have both displacements (local degree of freedom 1,2) and effective plastic strain (local degree of freedom 11) as fundamental unknowns while the last 4 nodes in the 8 noded elements should only have the displacement as fundamental unknowns. In the line for uel property all the property for the strain gradient dependent material is specified.

3.2 Postprocessing simulation based on the user element

An small UMat material subroutine

```
      SUBROUTINE UMAT(STRESS,STATEV,DDSDDE,SSE,SPD,SCD,
     1 RPL,DDSDDT,DRPLDE,DRPLDT,
     2 STRAN,DSTRAN,TIME,DTIME,TEMP,DTEMP,PREDEF,DPRED,CMNAME,
     3 NDI,NSHR,NTENS,NSTATV,PROPS,NPROPS,COORDS,DROT,PNEWDT,
     4 CELENT,DFGRD0,DFGRD1,NOEL,NPT,LAYER,KSPT,KSTEP,KINC)
C
      INCLUDE 'ABA_PARAM.INC'
      include 'kparameters.inc.f'
      include 'koutvar.inc.f'
      integer elemshift
C
      CHARACTER*80 CMNAME
      DIMENSION STRESS(NTENS),STATEV(NSTATV),DDSDDE(NTENS,NTENS),
     1 DDSDDT(NTENS),DRPLDE(NTENS),STRAN(NTENS),DSTRAN(NTENS),
     2 TIME(2),PREDEF(1),DPRED(1),PROPS(NPROPS),COORDS(3),DROT(3,3),
     3 DFGRD0(3,3),DFGRD1(3,3)
C
      elemshift=nint(props(1))

      do k1=1,ntens
       do k2=1,ntens
```

```
  DDSDDE(k1,k2)=0.0d0
 enddo
enddo

Stress(1)= sig11out(npt,noel-elemshift)
Stress(2)= sig22out(npt,noel-elemshift)
Stress(3)= sig33out(npt,noel-elemshift)
Stress(4)= sig12out(npt,noel-elemshift)

STATEV(1)= sigyout(npt,noel-elemshift)
STATEV(2)= epgradout(npt,noel-elemshift)
STATEV(3)= alphaout(npt,noel-elemshift)
STATEV(4)= Qgradout(npt,noel-elemshift)
STATEV(5)= tau1out(npt,noel-elemshift)
STATEV(6)= tau2out(npt,noel-elemshift)
RETURN
```

has been used in order to make a simple extraction of the state variable found in the Uel subroutine. By use the following lines in the input file

```
************ Visualizing *********************
*Element, type=cpe8, elset=output
*include, input=Out.elements.inp
*Solid section, Elset=output, Material=user
**Thickness
1.0e-6
*MATERIAL, NAME=user
*DEPVAR
6,
*USER MATERIAL,CONST=1
1000000
**************************************************
```

where the file "**Out.elements.inp**" is a copy of all the element definitions just with a high number (here 1000000) added to the element numbers. Thereby, it is possible to make visualization in a standard way in the ABAQUS/VIEWER.

4. Numerical results

4.1 Shearing a thin material layer between two rigid bounds

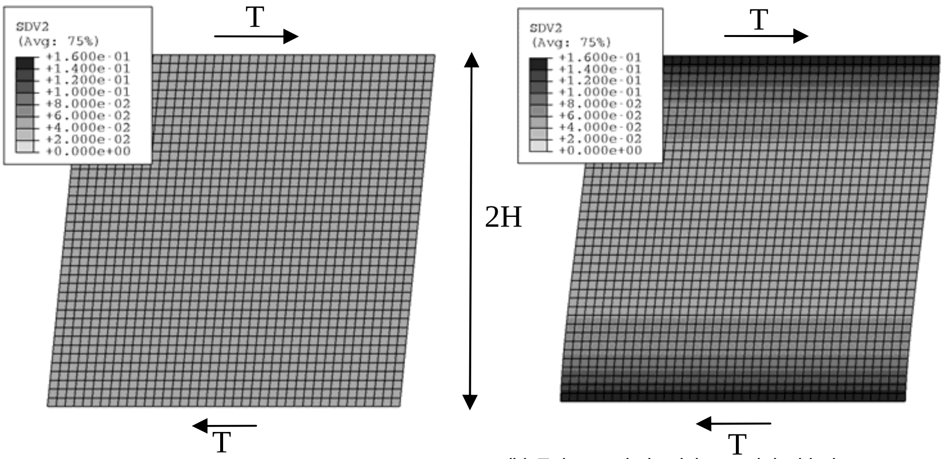

(a) Conventional plasticity model or an enhanced plasticity model with unconstrained plastic strains along the rigid boundary

(b) Enhanced plasticity model with the incorporated length scale $\ell_* = H$ with constrained plastic strains along the rigid boundary

Figure 1. Infinite wide slab sheared between two horizontal rigid boundaries.

Figure 1 show a solution of shearing an infinite wide thin layer of material between two rigid bounds. The problem has previous been analyzed analytically by Fleck and Hutchinson, 2001 and by a finite element model by Hutchinson and Niordson (2003). It is one of the simplest cases where it is possible to see an effect of the incorporated material length scale and is therefore used here as a test case. The slab is loaded under plane strain condition. The incorporated material length scale is normalized with the half thickness, H . Prescribing vanishing displacements in the vertical direction at all nodes in the finite element model corresponds to an infinity wide slab. In Figure 1, the deformation state predicted by conventional plasticity model (a) is compared with the deformation state predicted by the enhanced plasticity model (b) with a incorporated length scale given by $\ell_* = H$ (the one length scale version). The material is given by the yield stress $\sigma_y / E = 0.01$, Poisson's ratio $\nu = 0.3$ and the hardening exponent $n = 5$. Based on a conventional plasticity theory, a homogeneous solution will be predicted as seen in Figure 1a. This will also by the case in the strain gradient plasticity model with an incorporated length scale as long as the effective plastic strain is unconstrained along the rigid horizontal boundary. On the other hand, if plastic strains are prevented to develop along the rigid boundary, a boundary layer along the boundary will developed, see Figure 1b. The thickness of this boundary layer will depend on the incorporated material length scale. For a typical metal, this case corresponds to an elastic/elastic plastic material interfaces where the elastic material prevent the dislocations from the elastic plastic material to reach the interface and therefore form pile-ups. An effect which cannot be predicted using a conventional plasticity model. The contours on Figure 1 (SDV2) show the gradient dependent plastic strain E^P which is seen to be large at the boundary layer for non-vanishing length scale.

Figure 2 show the necessary shear traction in order to achieve a given overall shear strain in the infinite wide slab with a constrain plastic strain on the horizontal boundaries. Figure 2 show that a vanishing material length scale $\ell_* = 0$ coincide with the solution found using a conventional J2-flow theory. The J2-flow theory prediction is based on the standard 8-noded isoparametric element from the element library in ABAQUS. For a material with a larger incorporated length scale compared with the material thickness will give a stiffer response. “Small is stiff”.

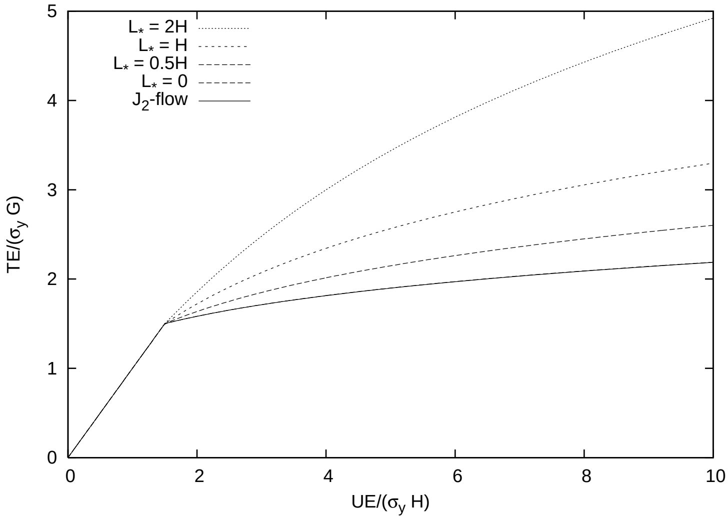

Figure 2. The shear response found for an infinite wide slab with full constrain of the plastic strain along the horizontal boundaries.

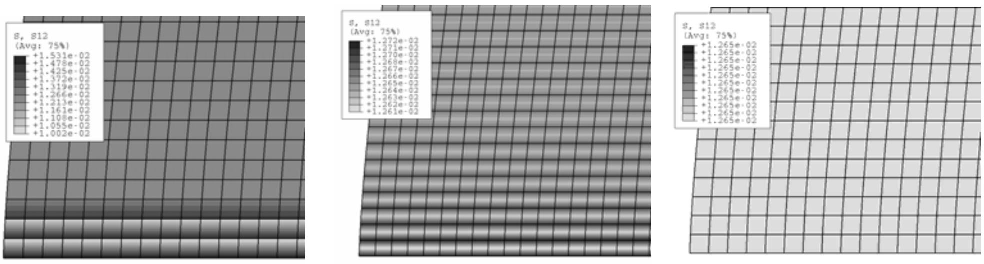

(a) 4-noded element with 2x2 Gauss integration points

(b) 8-noded element with 3x3 Gauss integration points

(c) Combined 4 and 8-noded element with 2x2 Gauss integration points

Figure 3. Zoom in on the bottom left corner of the contour plots of the shear stresses as a function of the chosen element type.

Figure 3 show a zoom in on the bottom left corner on the deformed mesh from Figure 1 now showing the contours of the shear stress. Both the strain gradient dependent model as well as the conventional model will predict a homogeneous stress state in the specimen, even though the shear stress will increase with a larger incorporated length scale. Nevertheless, figure 3 show locking phenomena for both a 4-noded and a 8-noded element. Instead, using the combined element which is a 8-noded element regarding the displacement and a 4-noded element regarding the effective plastic strain, an homogeneous solution is obtained.

4.2 Shearing a finite wide thin layer of material

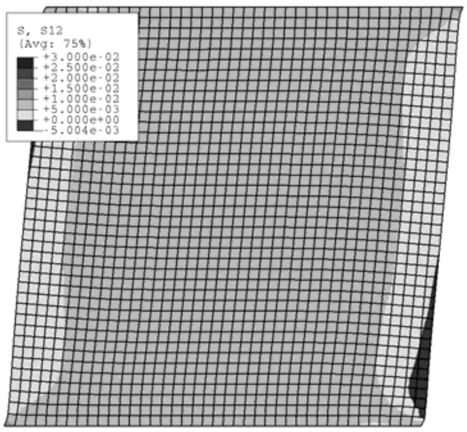

(a) Conventional plasticity model

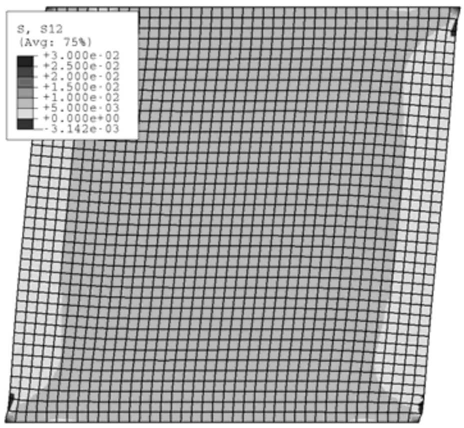

(b) Enhanced plasticity model $\ell_* = 0$

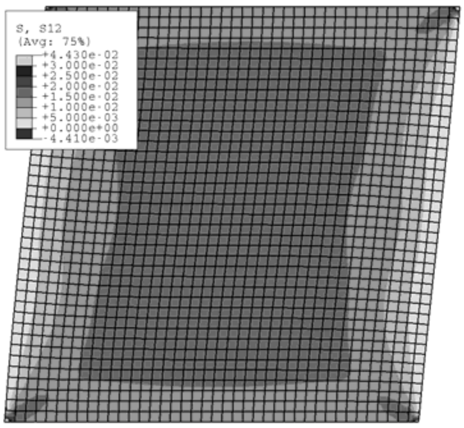

(c) Enhanced plasticity model with $\ell_* = H$

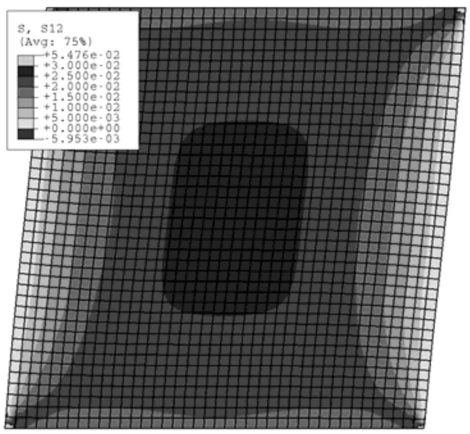

(d) Enhanced plasticity model with $\ell_1 = \ell_2 = \ell_3 = H$

Figure 4. A slab with a length to thickness ratio $L/H = 1$ sheared between two horizontal rigid materials with full constrain of the plastic strain along the horizontal boundaries

Figure 4 show the response for the similar case as simulated in Figure 1 but now for a slab with a finite width $W = H$. Compared with the infinite wide slab, this case is a little more complex to simulate, as the boundary between the instantaneous elastic and the instantaneous elastic-plastic material is moving throughout the simulation. The case is therefore will suited to study the influence of the boundary condition between this to regions. Figure 4 show that the prediction for $\ell_* = 0$ coincide with the prediction obtained using a conventional plasticity model. In addition the prediction from the one parameter strain gradient dependent plasticity model $\ell_* = H$ is compared with the strain gradient dependent plasticity model using three length scales. In Figure 4d the three length scale are chosen to be equal to each other.

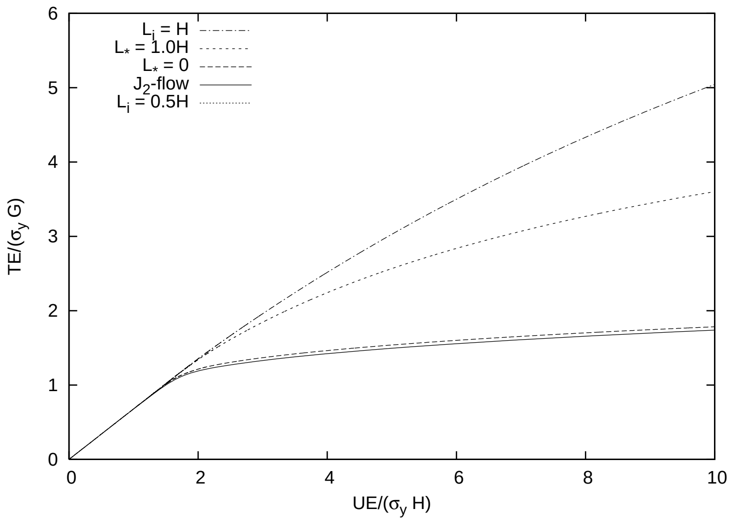

Figure 5. The shear response found for a finite wide slab $W / H = 1$ with full constrain of the plastic strain along the horizontal boundaries.

The normalized traction versus the deflection is shown in Figure 5. A stiffer response is again obtained for an increasing incorporated length scale. In Niordson and Tvergaard (2005) the influence of the internal elastic/elastic-plastic boundary is discussed. Niordson and Tvergaard (2005) incorporate either a vanishing higher order stress increment at the boundary $\dot{\tau} = 0$ by multiplying the "plastic element stiffness part", K_P from equation (5) with a small number in the elastic region. On the other hand, a internal boundary condition with a vanishing effective plastic strain increment, $\dot{\varepsilon}^P = 0$, is incorporated by multiplying K_P from equation (5) with a large number in the elastic region.

In the present work, the $\dot{\varepsilon}^P = 0$ at the internal elastic/elastic-plastic boundary is used for all cases. Here, the boundary condition is insured by setting the materials hardening modulus from equation (3) equal to a sufficiently large number. Figure 6 show that choosing a number larger than $h_E = 10^3 E$ will give a converging solution.

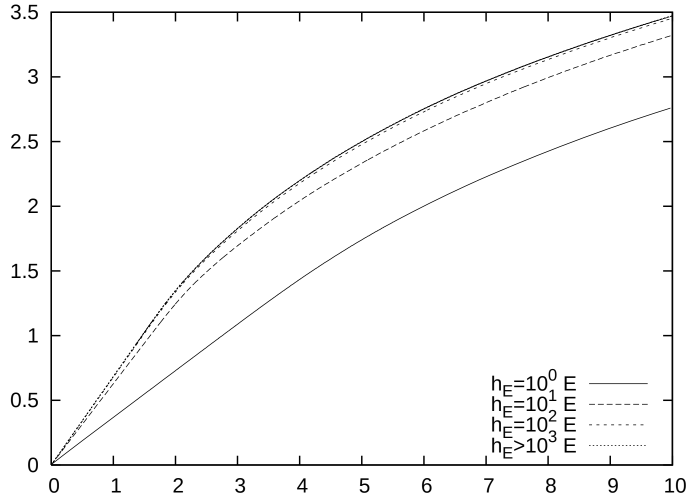

Figure 6. The shear response found for a finite wide slab $W/H = 1$ with full constrain of the plastic strain along the horizontal boundaries.

4.3 Crack tip simulations

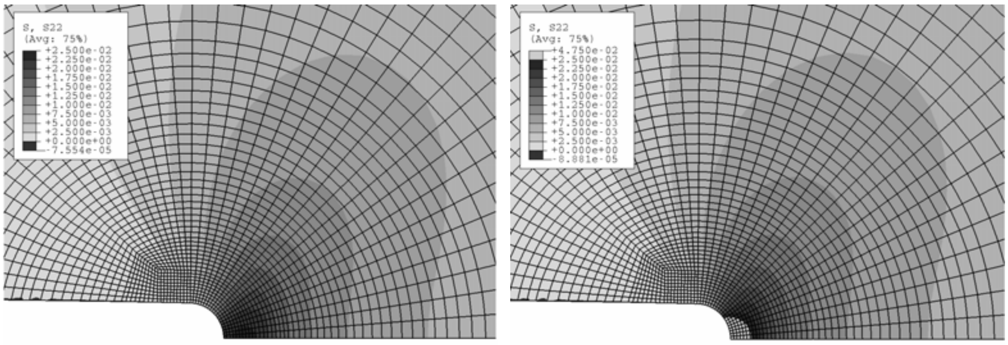

(a) $\ell_* = 0.1R_{tip}$ (b) $\ell_* = R_{tip}$

Figure 7. The contours of the horizontal stress components σ_{22}

Figure 7 show the crack opening stress components at the crack top for a pure mode one loaded crack tip at an infinite large specimen. For an increasing incorporated length scale compared with the crack tip radius the stress concentration is seen to move towards the crack tip surface and the value for a given prescribed K_I -value is seen to increase. The opposite is seen to be the case for the effective plastic strain. For increasing incorporated length scales, the maximum value of the effective plastic strain is seen to decrease and the point with the maximum plastic strain is seen to move away from the crack tip surface.

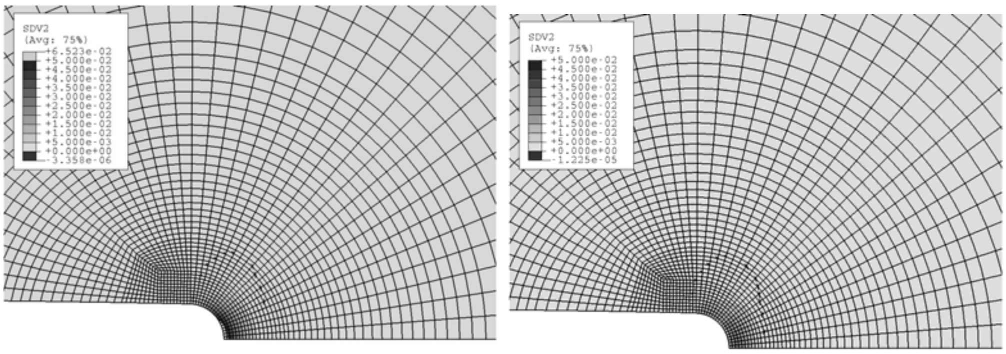

(a) $\ell_* = 0.1R_{tip}$ (b) $\ell_* = R_{tip}$

Figure 8. The contours of the gradient dependent effective plastic strain E^P

5. Conclusion

The advanced by implementing the model in ABAQUS:

- Address a large range of problem
- Apply the theory to models already implemented using standard ABAQUS elements
- Use together with other elements already available in ABAQUS
- Exchange elements/material models with students and co-workers
- Using the pre- and post processing facility in ABAQUS

6. References

1. Acharya, A., Basssani, J.L., 2000. Incompatibility and crystal plasticity. Mech. Phys. Solids 48, 1565-1595
2. Aifantis, E.C., 1984. On the microstructural origin of certain inelastic models. Trans. ASME J. Eng. Mat Tech. 106, 326-330
3. Fleck, N.A., Hutchinson, J.W., 1997. Strain gradient plasticity. In: Hutchinson, J.W., Wu, T.Y. (Eds.), Advances in Applied Mechanics, Vol. 33. Academic Press, New York, pp. 295-361.
4. Fleck, N.A. and J.W. Hutchinson, “A reformulation of strain gradient plasticity theory,” Journal of Mechanics and Physics of Solids, Vol. 49, pp. 2245-2271, 2001.
5. Fleck, N.A., Muller, G.M, Ashby, M.F. and Hutchinson, J.W. Strain gradient plasticity: Theory and experiment. Acta Metallurgica et Materialia, Vol 42, 475-487, 1994
6. Stelmashenko, N. A., M. G. Walls, L. M. Brown and Yu. V. Milman, Microindentations on W and Mo oriented single crystals: An STM study, Acta Metallurgica et Materialia, 41, 2855-2865, 1993.
7. Mikkelsen, L.P. “Crack-growth in a strain gradient dependent plasticity model,” Proceedings of the 19th Nordic Seminar on Computational Mechanics, Lund, 20-21 October, 2006.
8. Niordson, C.F. and J.W. Hutchinson, “Non-uniform plastic deformation of micron scale objects. International Journal Numerical Methods in Engineering, Vol. 56, 961-975, 2003.
9. Niordson, C.F. and Tvergaard, V. Instabilities in power law gradient hardening materials. International Journal of Solids and Structures 42, 2005-2573.

7. Acknowledgement

The author wishes to thank Professor John W. Hutchinson for many valuable discussions during the course of this work and as my host on a 3 month visiting scholarship at Harvard University.

The work has been financial supported by the Danish Technical Research Council in a project entitled “Modeling Plasticity at the Micron Scale”.